

# A new transmissometer method that measures runway visibility across a short distance

Mariam Mohamed Abud

Department of Physics, College of Education, Mustansiriyah University, Baghdad, Iraq

## Article Info

### Article history:

Received Nov 24, 2022

Revised Mar 4, 2023

Accepted Apr 12, 2023

### Keywords:

Dust

Raindrops

Runway visual range

Transmissometer

Visibility

## ABSTRACT

The present technique developed a transmissometer idea for intensity measurements in the ecosystem across an 80 cm distance. The method relies on the transmission of an optical or infrared (diode laser 785 nm) signal obtained on spectrum analyses (ocean optics HG4000) received signal from the laser under unique conditions (light dust, heavy dust, and waterdrops) at a short distance. Thus, this approach is useful to measure the intensities of the laser beam and locate the visibility measurements of laser transmissometers in the rain and special care to the dust. The results showed that heavy dust enhanced the visibility measurements for distinct intensity distributions between showers and dust. Since light and heavy dust within a single transmittance can easily cover the entire runway visual range (RVR) range for a brief period, visibility measurements were crucial. The full-scale value corresponds to infinite visibility for heavy dust (0.8611) and minimum visibility for drop rain conditions (0.01073).

This is an open access article under the [CC BY-SA](#) license.



## Corresponding Author:

Mariam Mohamed Abud

Department of Physics, College of Education, Mustansiriyah University

Baghdad, Iraq

Email: marmoh\_1968@uomustansiriyah.edu.iq

## 1. INTRODUCTION

Changes in signal transmission over short distances under climatic conditions like high dust and rain were necessary because of recent climatic shifts in our region and the rest of the world. Recent moderate climatic fluctuations necessitate a thorough scientific investigation of how the environment affects communications and the transmission of optical indicators over long and short distances. Aerosol is a dispersion of tiny solid or liquid particles in the atmosphere [1]. The front-end units and components needed to implement them, as well as the design studies and simulation model of a digital fiber communication system employing (optisystem.10), are all examined. The system is configured to its best advantage using the laser transmitter's (1310 nm and 1550 nm) [2] wavelengths as input power (dBm), the optical fiber's (SM and MM) cable types as channel length (km), and the (return to zero (RZ) and non-return to zero (NRZ)) modulation and demodulation schemes to maximize spectral efficiency and power efficiency by encoding information. These settings are then analyzed to determine how they affect the receiver's signal quality [2], [3].

It discusses the types of fibers used in the optical fiber communication system as well as the basic communication concept. Several fundamental ideas have been clarified that will impact the system's effectiveness. Addition, an aerosol in the atmosphere is concentrated enough to be seen. Although the particles are too minute to be seen individually, they nonetheless work to limit the viewing field. Dust is an exceptional powder made up of very small portions of earth or sand [4]. Additionally, fringe visibility is generally recognized as one of the key factors impacting how accurately interferometers measure [3]–[30].

Atmospheric visibility descent is essential environmental trouble in China because of the massive extent of aerosol emissions [31]–[36].

The atmospheric visibility and turbulence optical meter (AVTOM) use a transmission technique to simultaneously measure the atmosphere's visibility and intensity of turbulence. Air visibility is measured using the extinction principle, and the concept of light intensity flicker is utilized to calculate the intensity of turbulence [37]. A synchronous dimension device for atmospheric visibility and turbulence depth is created together with its theory, graph, and experiments [38], [39]. Furthermore, an experimental free space optics (FSO) system's visibility measurement choices are evaluated, and attenuation coefficients for optical wireless at various laser wavelengths are compared (632 nm, 785 nm, 1310 nm, and 1550 nm) [40], [41]. Therefore, it must estimate the visibility of experimental patterns to produce the interference patterns with the highest visibility. Meanwhile, we create the fourier-polar transform and combine it with the directional projection to determine the carrier fringe pattern's overall visibility [42].

3D measurement has seen a lot of research on fringe projection profilometry (FPP) [43]. Thus, new opportunities to effectively observe current visibility and cloud coverage/height using a camera-based observation system [44]. In light of the climatic fluctuations that our planet earth suffers from and its repercussions and problems by sending visual signals using the spectra analyzer within short ranges, so the goal in this research is to develop a runway visual way method within a short range for transmissometer and to find visibility as it is important in transmission standards at airports.

## 2. THEORETICAL OF TRANSMISSOMETER FOR THE VISIBILITY MEASUREMENT

The depth of monochromatic light transmitted over a preset channel length is measured using an optical instrument called a transmissometer. Meanwhile, visibility deuteriation is measured with a transmissometer device. After applying math to calculate visibility, we may then determine the runway visual range (RVR) and metrological optical range (MOR) [45]–[47]. The crucial climatic parameter, particularly the transparency of the atmosphere, known as the RVR, may be measured objectively. There are two different kinds of transmissometers as shown in Figure 1 [4], i) those with a transmitter and a receiver in separate units and spaced at a known distance from one another, as shown in Figure 1(a) and ii) those with a transmitter and a receiver in the same unit, with the emitted light reflected by a remote mirror or retroreflector (the light beam traveling to the reflector and back), as shown in Figure 1(b). The transmittance range of the transmissometer is from 0 to 1, with 0 (zero) as the baseline.

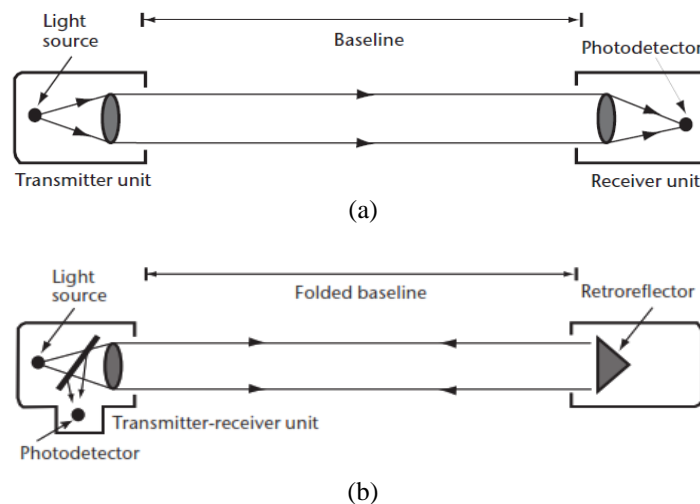


Figure 1. Types of transmissometers: (a) a transmissometer with two ends and (b) a transmissometer with one end

### 2.1. Rule of fringe visibility

A two-beam typical fringe pattern represented mathematically interfering factors include [48], [49]:

$$I_{res} = I_1 + I_2 \pm 2\sqrt{I_1 I_2} \cos \theta \quad (1)$$

where  $I_1$  and  $I_2$  represent the distribution of the intensity of the and is the phase difference  $\Theta$  between the two respective waves (interfering waves).

A type of interference, in terms of the amplitude, envelop of the fringe intensity, and the average intensity over a given space domain that is the simple density diluted through dust or drop of rain particles is  $I_{\min}$  and most intensity passes free area  $I_{\max}$ , and the visibility  $V$  is defined [50], [51]:

$$V = \frac{\Delta I}{I_{\max} + I_{\min}} \quad (2)$$

where,  $\Delta I$ : the difference in intensities,  $I_{\max}$ : max. of intensity ( $\text{w/m}^2$ ),  $I_{\min}$ : the min. of depth ( $\text{w/m}^2$ ). The degree of source coherence, the length difference, and the visibility all affect visibility. The full-scale 1 (unity) value corresponds to infinite visibility and zero visibility [52].

### 3. RESEARCH METHOD

The chamber glass that is used to execute the lab test symbolizes the system of climate effect on the sign: (i) Light supply (785 nm); ii) Chamber glass rooms used to represent, this chamber needs to have the functionality to lead to similar weather conditions droplet, light, and heavy dust. The glass chamber should be equipped with a water sprayer controlled using an external water pump to function under the circumstance state. In addition, the glass room must incorporate a facet fan to spread the soil in the rooms to operate a dust state; and iii) Ocean optic machine spectrometer machine analyzer instrument for an obtained sign that can detect the received spectrum light. Then, translate it to the laptop with the use of a USP connector. Afterward, ocean optic software in the laptop attracts the spectrum of the mild. The graph is shown in decide Figure 2.

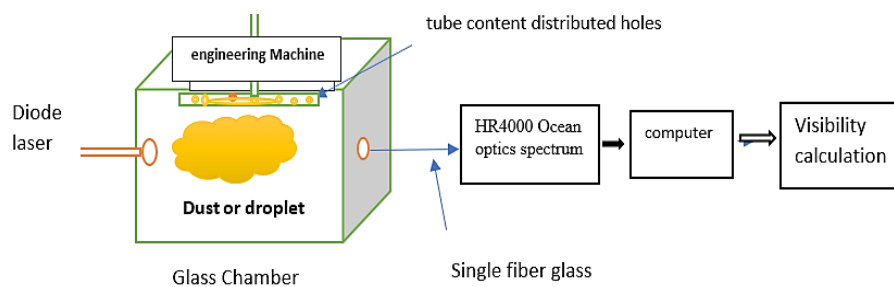


Figure 2. A method of transmissometer for the visibility measurement diagram

Figure 3 represents how the equipment's arranged to shape the simple transmitter system. Herein, laser led commenced to emit his laser beam through the glass room "chamber" which in flip carried out the character istic of air effect. Then, after accomplishing the receiver side, the ocean optics spectrum detector receives the light and internally translates it to the pc using the serial peripheral interface connector. The visibility relies upon the diploma of coherence of the source. There is a significant difference in the length of the paths, just as there is with respect to the feature of the spectrum analyzer with regard to the laser supply through a chamber glass that has an 80 cm dimension.

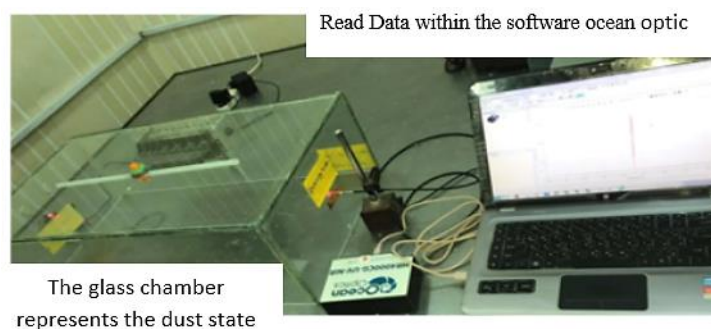


Figure 3. Experimental device to calculate the visibility

#### 4. RESULTS AND DISCUSSION

The ocean optic software reads the receives signal and appears it via the software through a plot that offers the relation between the depth count number of mild and the type of wavelength that was once used in the experiment.

##### 4.1. The impact of heavy and light dust on measurements of visibility

The ocean optic software reads the receives signal and appears it via the software through a plot that offers the relation between the depth count number of mild and the type of wavelength that was once used in the experiment. The output laser 785 nm beam from the used optics spectrum software (HR4000), offers the relation between depth versus wavelength, as demonstrated in Figure 4. Meanwhile, Figure 5 suggests less depth in the presence of moderate (light dust) with the identical laser beam.

The capacity depth on the same aerosol's increased dust generated a drop in incident laser depth to the value ( $I_{\min}=1223$ ) for the laser's intensity, as shown in Figure 6, in order to determine how to increase the dirt's impact on the incident laser beam. When compared to average visibility, low visibility indicates that the particle concentration and size are both higher. So, in poor visibility situations, scattering and attenuation may be more pronounced. Visibility is measured by calculating the amount of light that is attenuated by atmospheric particles (smoke, dust, haze, fog, rain, and snow) as they pass through the particle size [53]. Experimental findings showing attenuation in vision function. Meteorological factors like geometric attenuation and air attenuation have a substantial impact on FSO link performance [54], [55].

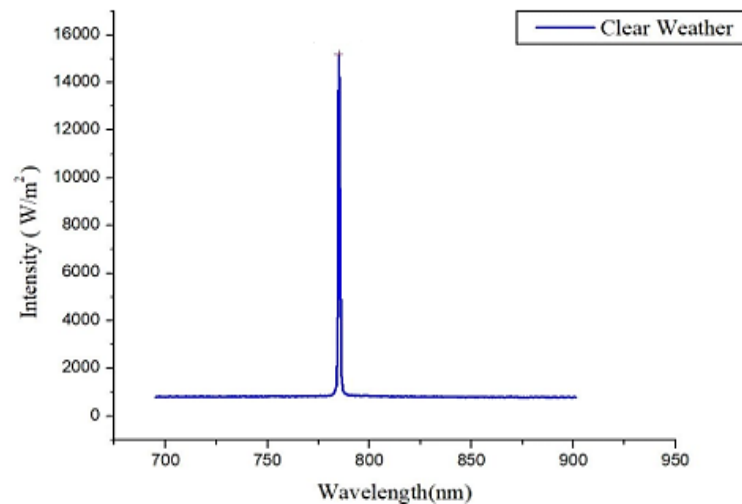


Figure 4. The signal laser represents  $I_{\max}$  (at  $\lambda=785$  nm) in clean inside chamber glass

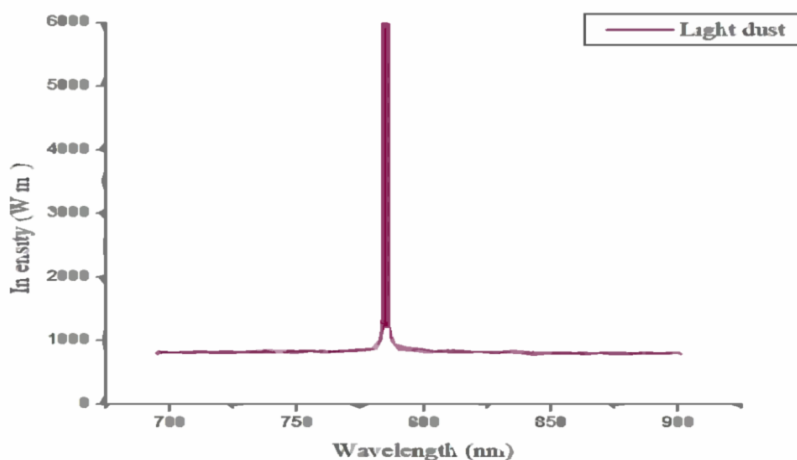


Figure 5. The attenuation of the intensity ( $I_{\min}$ ) vs. wavelength in (785 nm) with light dust

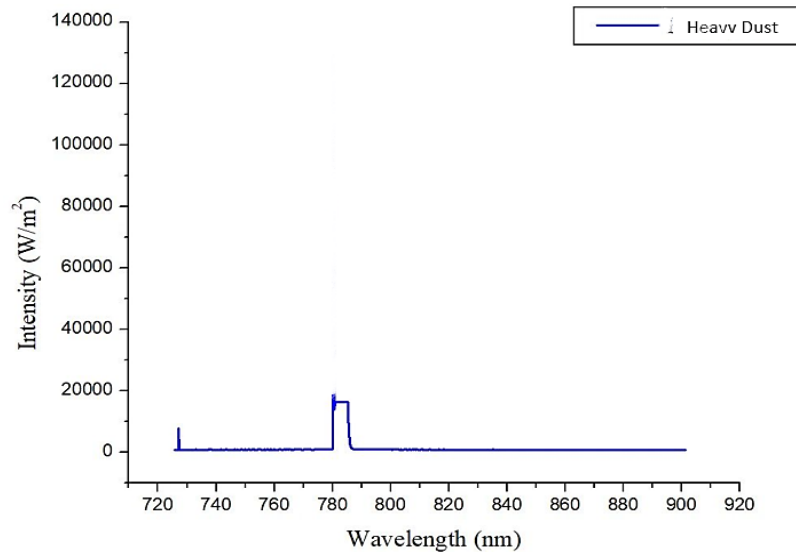


Figure 6. The intensity vs. wavelength of 785 nm with heavy dust

#### 4.2. The effects of raindrops on visibility measures

When consequences had been compared to all-weather effects, thus indicating that raindrops are much less effective using dirt on visibility measurements when calculating the visibility in (2) for light dust, heavy dust, and raindrops. From Table 1, the strategy used to degree the permeability within the transmitter meter is imperative within the case of tidy thickness and the increment of its particles more than light dust, as a result of the weakening of the escalated through the tidy particles of light dust that must be taken into consideration by applying an equation over a short distance of 80 cm.

Raindrops also didn't seem to have as much of an impact on visibility as they did in the dust with the new design. Meanwhile, the particle concentration and size are higher than what is expected for visibility. Thus, low visibility conditions may result in increased scattering [56] and attenuation [57]. The RVR or meteorological optical range is the term used to describe the fundamental meteorological quantity, which is the transparency of the atmosphere. Visibility RVR, a method has been proven through previous studies with the limits of kilometers, but the transmissometer using spectrum analyser has a receiver used in our current research has proven to measure the visibility, which during short distance.

Table 1. Summary of the visibility was calculated for different conditions at max. intensity  $I_{\max}=16383 \text{ w/m}^2$  using laser diode beam (784.97 nm)

Weather	Intensity(w/m <sup>2</sup> )	Visibility	Visibility%
Light dust	5787	0.478	47.8
Heavy dust	1223	0.8611	86.11
Raindrops	16035	0.01073	1.07

#### 5. CONCLUSION

In this work, the visibility dimension uses the transmissometer method or a novel method. The visibility used is soon calculated for particular optical course distributions of rain and dust, which is increasing with the extended dust. Therefore, in this method, show that: i) the depth of every case of dust minimized heavily relative to the whole obtained intensity of the laser beam, ii) the method is particularly useful for fringe construct (visibility) patterns that frequently emerge in interferometric experiments, such as low contrast low-intensity heavy dust, and increased intensity in raindrops at a short period, and iii) the laser transmissometer's visibility measurements at close range raise significance regarding the laser transmissometer's optical structures at less than one meter away. So, for a transmissometer with two ends, the influence of heavy dust on the dimension of visibility is greater than the impact of raindrops within this close range.

## ACKNOWLEDGEMENTS




I would like to acknowledge, Dr. Asmaa Roof and Hashem, Jaber, College of Education, Mustansiriyah University

## REFERENCES

- [1] J. A. Kalati, "Design study of adaptive optics technique of the FSO communication system," *Journal of College of Education*, no. 3, pp. 31–42, 2018.
- [2] S. A. Kadhim, Z. A. Saleh, A. M. Raoof, and A. T. Lateef, "Design study and simulation of a digital fiber communication system using (optisystem.10)," *International journal of engineering sciences & research technology*, vol. 5, no. 8, pp. 952–959, Aug. 2016, doi: 10.5281/ZENODO.60837.
- [3] S. A. Kadhim, Z. A. Saleh, and A. M. Raoof, "Performance evaluation of experimental digital optical fiber communication link," *International Journal of Innovative Research in Science, Engineering and Technology*, vol. 6, no. 10, pp. 19534–19543, Oct. 2017, doi: 10.15680/IJRSET.2017.0610054.
- [4] World Meteorological Organization, "Guide to meteorological instruments and methods of observation," *World Meteorological Organization Geneva, Switzerland*, vol. WMO-No. 8, no. Chapter 9, pp. 1–14, 2006, doi: 10.25607/OBP-432.
- [5] S. A. Ackerman *et al.*, "Satellites see the world's atmosphere," *Meteorological Monographs*, vol. 59, no. 1, pp. 4.1-4.53, Jan. 2019, doi: 10.1175/AMSMONOGRAPHIS-D-18-0009.1.
- [6] J. M. Apke, K. A. Hilburn, S. D. Miller, and D. A. Peterson, "Towards objective identification and tracking of convective outflow boundaries in next-generation geostationary satellite imagery," *Atmos. Meas. Tech.*, vol. 13, no. 3, pp. 1593–1608, Apr. 2020, doi: 10.5194/amt-13-1593-2020.
- [7] B. Bartlett, J. Casey, F. Padula, A. Pearlman, D. Pogorzala, and C. Cao, "Independent validation of the advanced baseline imager (ABI) on NOAA's GOES-16: post-launch ABI airborne science field campaign results," vol. 10764, Sep. 2018, doi: 10.1117/12.2323672.
- [8] M. Bauwens *et al.*, "Impact of coronavirus outbreak on NO<sub>2</sub> pollution assessed using TROPOMI and OMI observations," *Geophysical Research Letters*, vol. 47, no. 11, Jun. 2020, doi: 10.1029/2020GL087978.
- [9] K. Bedka, E. M. Murillo, C. R. Homeyer, B. Scarino, and H. Mersiovsky, "The above-anvil cirrus plume: an important severe weather indicator in visible and infrared satellite imagery," *Weather and Forecasting*, vol. 33, no. 5, pp. 1159–1181, Oct. 2018, doi: 10.1175/WAF-D-18-0040.1.
- [10] T. M. Bell, B. R. Greene, P. M. Klein, M. Carney, and P. B. Chilson, "Confronting the boundary layer data gap: evaluating new and existing methodologies of probing the lower atmosphere," *Atmos. Meas. Tech.*, vol. 13, no. 7, pp. 3855–3872, Jul. 2020, doi: 10.5194/amt-13-3855-2020.
- [11] R. J. Blakeslee *et al.*, "Three years of the lightning imaging sensor onboard the international space station: expanded global coverage and enhanced applications," *JGR Atmospheres*, vol. 125, no. 16, Aug. 2020, doi: 10.1029/2020JD032918.
- [12] K. Brewster, A. Bajij, B. Philips, D. Pepyne, E. Lyons, and F. Carr, "CASA dallas-fort worth urban testbed observations: networks of networks at work," in *Presented at the Special Symposium on Meteorological Observations and Instrumentation*, Seattle, WA, Jan. 2017, pp. 1–11.
- [13] F. V. Brock and S. J. Richardson, *Meteorological measurement systems*. Oxford University Press, 2001, doi: 10.1093/oso/9780195134513.001.0001.
- [14] J. A. Brotzge *et al.*, "A technical overview of the New York state mesonet standard network," *Journal of Atmospheric and Oceanic Technology*, vol. 37, no. 10, pp. 1827–1845, Oct. 2020, doi: 10.1175/JTECH-D-19-0220.1.
- [15] K. Chance, X. Liu, R. M. Suleiman, D. E. Flittner, J. Al-Saadi, and S. J. Janz, "Tropospheric emissions: monitoring of pollution (TEMPO)," *presented at the SPIE Optical Engineering + Applications*, J. J. Butler, X. (Jack) Xiong, and X. Gu, Eds., San Diego, California, United States, Sep. 2013, doi: 10.1117/12.2024479.
- [16] P. B. Chilson *et al.*, "Moving towards a network of autonomous UAS atmospheric profiling stations for observations in the earth's lower atmosphere: the 3D mesonet concept," *Sensors*, vol. 19, no. 12, Jun. 2019, doi: 10.3390/s19122720.
- [17] T. Foken, *Micrometeorology*. Berlin, Heidelberg: Springer Berlin Heidelberg, 2017, doi: 10.1007/978-3-642-25440-6.
- [18] T. Foken, Ed., *Springer handbook of atmospheric measurements*, in Springer Handbooks. Cham: Springer International Publishing, 2021, doi: 10.1007/978-3-030-52171-4.
- [19] A. J. Geer, S. Migliorini, and M. Matricardi, "All-sky assimilation of infrared radiances sensitive to mid- and upper-tropospheric moisture and cloud," *Atmos. Meas. Tech.*, vol. 12, no. 9, pp. 4903–4929, Sep. 2019, doi: 10.5194/amt-12-4903-2019.
- [20] R. G. Harrison, *Meteorological measurements and instrumentation*, 1st ed. Wiley, 2014, doi: 10.1002/9781118745793.
- [21] T. Horton, M. Bolt, C. Prather, J. Manobianco, and M. L. Adams, "Airborne sensor network for atmospheric profiling," *WSN*, vol. 10, no. 04, pp. 93–101, 2018, doi: 10.4236/wsn.2018.104005.
- [22] A. J. Illingworth *et al.*, "How can existing ground-based profiling instruments improve european weather forecasts?," *Bulletin of the American Meteorological Society*, vol. 100, no. 4, pp. 605–619, Apr. 2019, doi: 10.1175/BAMS-D-17-0231.1.
- [23] K. D. Klaes *et al.*, "The EUMETSAT polar system: 13+ successful years of global observations for operational weather prediction and climate monitoring," *Bulletin of the American Meteorological Society*, vol. 102, no. 6, pp. E1224–E1238, Jun. 2021, doi: 10.1175/BAMS-D-20-0082.1.
- [24] S. Liang, *Comprehensive remote sensing - 1st edition*, 1st Edition. New York, United States: Elsevier, 2017.
- [25] W. P. Menzel, T. J. Schmit, P. Zhang, and J. Li, "Satellite-based atmospheric infrared sounder development and applications," *Bulletin of the American Meteorological Society*, vol. 99, no. 3, pp. 583–603, Mar. 2018, doi: 10.1175/BAMS-D-16-0293.1.
- [26] R. E. Morss, K. A. Emanuel, and C. Snyder, "Idealized adaptive observation strategies for improving numerical weather prediction," *Journal of the Atmospheric Sciences*, vol. 58, no. 2, pp. 210–232, Jan. 2001, doi: 10.1175/1520-0469(2001)058<0210:IAOSFI>2.0.CO;2.
- [27] A. Nag, M. J. Murphy, W. Schulz, and K. L. Cummins, "Lightning locating systems: Insights on characteristics and validation techniques," *Earth and Space Science*, vol. 2, no. 4, pp. 65–93, Apr. 2015, doi: 10.1002/2014EA000051.
- [28] S. M. Spuler, K. S. Repasky, B. Morley, D. Moen, M. Hayman, and A. R. Nehrir, "Field-deployable diode-laser-based differential absorption lidar (DIAL) for profiling water vapor," *Atmospheric Measurement Techniques*, vol. 8, no. 3, pp. 1073–1087, Mar. 2015, doi: 10.5194/amt-8-1073-2015.
- [29] World Meteorological Organization, "Guide to instruments and methods of observation," *World Meteorological Organization Geneva, Switzerland*, vol. WMO-No. 8, no. Chapter 9, 2018, doi: 10.25607/OBP-432.

- [30] H. B. Bluestein, F. H. Carr, and S. J. Goodman, "Atmospheric observations of weather and climate," *Atmosphere-Ocean*, vol. 60, no. 3–4, pp. 149–187, Aug. 2022, doi: 10.1080/07055900.2022.2082369.
- [31] K. Du, C. Mu, J. Deng, and F. Yuan, "Study on atmospheric visibility variations and the impacts of meteorological parameters using high temporal resolution data: an application of Environmental Internet of Things in China," *International Journal of Sustainable Development & World Ecology*, vol. 20, no. 3, pp. 238–247, Jun. 2013, doi: 10.1080/13504509.2013.783886.
- [32] Y. Cui, C. Wei, Y. Zhang, F. Wang, and Y. Cai, "Effect of the atmospheric turbulence on a special correlated radially polarized beam on propagation," *Optics Communications*, vol. 354, pp. 353–361, Nov. 2015, doi: 10.1016/j.optcom.2015.06.017.
- [33] J. Zhao, S. Xiao, X. Wu, and X. Zhang, "Parallelism detection of visibility meter's probe beam and the effect on extinction coefficient measurement," *Optik*, vol. 128, pp. 34–41, Jan. 2017, doi: 10.1016/j.ijleo.2016.09.119.
- [34] L. Mei, P. Guan, Y. Yang, and Z. Kong, "Atmospheric extinction coefficient retrieval and validation for the single-band Mie-scattering Scheimpflug lidar technique," *Opt. Express*, vol. 25, no. 16, Aug. 2017, doi: 10.1364/OE.25.00A628.
- [35] J. Guo *et al.*, "Declining frequency of summertime local-scale precipitation over eastern China from 1970 to 2010 and its potential link to aerosols," *Geophysical Research Letters*, vol. 44, no. 11, pp. 5700–5708, 2017, doi: 10.1002/2017GL073533.
- [36] Y. Han *et al.*, "Ground-based synchronous optical instrument for measuring atmospheric visibility and turbulence intensity: theories, design and experiments," *Opt. Express*, vol. 26, no. 6, pp. 6833–6850, Mar. 2018, doi: 10.1364/OE.26.006833.
- [37] A. Basahel, I. Md. Rafiqul, M. H. Habaebi, and A. Z. Suriza, "Visibility effect on the availability of a terrestrial free space optics link under a tropical climate," *Journal of Atmospheric and Solar-Terrestrial Physics*, vol. 143–144, pp. 47–52, Jun. 2016, doi: 10.1016/j.jastp.2016.03.005.
- [38] T. Czarnecki, K. Perlicki, and G. Wilczewski, "Atmospheric visibility sensor based on backscattering using correlation coding method," *Opt Quant Electron*, vol. 47, no. 3, pp. 771–778, Mar. 2015, doi: 10.1007/s11082-014-9951-x.
- [39] R. Babari, N. Hautière, É. Dumont, R. Brémond, and N. Paparoditis, "A model-driven approach to estimate atmospheric visibility with ordinary cameras," *Atmospheric Environment*, vol. 45, no. 30, pp. 5316–5324, Sep. 2011, doi: 10.1016/j.atmosenv.2011.06.053.
- [40] M. Márton, L. Ovseník, T. Huszaník, and M. Špes, "Analysis of possibilities for measurement effect of visibility in experimental FSO system," *Open Computer Science*, vol. 8, no. 1, pp. 135–141, Jul. 2018, doi: 10.1515/comp-2018-0013.
- [41] M. M. Abud, J. A. Akhlali, and A. M. Roof, "Comparison of attenuation coefficient at different lasers 632, 785 nm, 1310 nm and 1550 nm in Dust for optical wireless," *J. Phys.: Conf. Ser.*, vol. 1795, no. 1, Mar. 2021, doi: 10.1088/1742-6596/1795/1/012014.
- [42] B. Fu-zhong, J. Chen, X. Gao, and Y. Xu, "Estimation technique of global fringe visibility using in interferometers with adjustable visibility," In *Research Square*, Aug. 2020, doi: 10.21203/rs.3.rs-58924/v1.
- [43] S. Yang, H. Huang, G. Wu, Y. Wu, T. Yang, and F. Liu, "High-speed three-dimensional shape measurement with inner shifting-phase fringe projection profilometry," *Chin. Opt. Lett.*, vol. 20, no. 11, Nov. 2022.
- [44] J. Bartok, L. Ivica, L. Gaál, I. Bartoková, and M. Kelemen, "A novel camera-based approach to increase the quality, objectivity and efficiency of aeronautical meteorological observations," *Applied Sciences*, vol. 12, no. 6, Jan. 2022, doi: 10.3390/app12062925.
- [45] C. E. Dorman, "Early and recent observational techniques for fog," in *Marine Fog: Challenges and Advancements in Observations, Modeling, and Forecasting*, D. Koračin and C. E. Dorman, Eds., in Springer Atmospheric Sciences. Cham: Springer International Publishing, 2017, pp. 153–244, doi: 10.1007/978-3-319-45229-6\_3.
- [46] H. Davate, L. Bhadavkar, S. Jangam, and Ms. N. Nagdeo, "Runway visibility measurement using transmissometer," *International Journal of Scientific Research and Review*, vol. 8, no. 5, pp. 1319–1321, 2019.
- [47] W. S. Kessler, S. E. Wijffels, S. Cravatte, N. Smith, and Lead Authors, "Second report tropical pacific observing system 2020," *GOOS-234*, pp. 1–243, 2019.
- [48] F. Pedrotti and L. Pedrotti, *Introduction to optics*, 2nd ed. in Chapter 10. London: Prentice-Hall, 1993.
- [49] *Manual of runway visual range observing and reporting practices*, Third Edition. International Civil Aviation Organization, 2005.
- [50] A. G. Alkholidi and K. S. Altowij, "Free space optical communications — theory and practices," in *Contemporary Issues in Wireless Communications*, M. Khatib, Ed., 1st edition. in Chapter 5. InTech, 2014, pp. 159–212, doi: 10.5772/58884.
- [51] G. Rajshekhar and P. Rastogi, "Fringe analysis: premise and perspectives," *Optics and Lasers in Engineering*, vol. 50, no. 8, pp. iii–x, Aug. 2012, doi: 10.1016/j.optlaseng.2012.04.006.
- [52] Q. Wang *et al.*, "Microphysics and optical attenuation in fog: observations from two coastal sites," *Boundary-Layer Meteorol*, vol. 181, no. 2, pp. 267–292, Dec. 2021, doi: 10.1007/s10546-021-00675-5.
- [53] B. S. S. Naimullah, S. Hitam, N. S. M. Shah, M. Othman, S. B. A. Anas, and M. K. Abdullah, "Analysis of the effect of haze on free space optical communication in the Malaysian environment," in *2007 IEEE International Conference on Telecommunications and Malaysia International Conference on Communications*, May 2007, pp. 391–394, doi: 10.1109/ICTMICC.2007.4448669.
- [54] F. K. Shaker, "Design, implementation and performance enhancement study of a wireless full-optical free space communication system," M. Thesis in Physics, Dep. of Physics, College of Education, Mustansiriyah University, Baghdad., Iraq, 2017.
- [55] F. A. Kareem, "Study the attenuation of the atmospheric effects on laser beam (875, 850, 1550) nm in free space propagation," Ph.D. dissertation, Dep. of Physics, College of Education, Mustansiriyah University, Baghdad., Iraq, 2008.
- [56] M. M. Abud, "Measure of backscatter for small particles of atmosphere by lasers," *J. Phys.: Conf. Ser.*, vol. 1003, May 2018, doi: 10.1088/1742-6596/1003/1/012079.
- [57] H. A. Jabar, R. A. Fayadh, and M. M. Abud, "Investigation of rain and haze attenuations impact on proposed SCM-SAC-OCDMA-FSO system with optical amplifier," *IJACR*, vol. 8, no. 39, pp. 342–353, Nov. 2018, doi: 10.19101/IJACR.2018.839004.

**BIOGRAPHIES OF AUTHOR**

**Mariam Mohamed Abud**    the Ph.D. degree in Physics, exact jurisdiction laser, and optics, is teaching at the Mustansiriyah University, College of Education, Department of Physics. She worked as a lecturer in the Faculty of Science and Science for girls in the Department of Physics, University of Baghdad, she has worked as a lecturer and lecturer since 1990 at the College of Science, Department of Physics, University of Baghdad. She was appointed to the University of Basra, College of Engineering, Department of Materials Engineering (2007-2009). She has a patent from the standardization and quality control in Department of Patents and is a member of the Iraqi inventors association patents 63193031, from US patent to the USPTO for a novel method of medical communication that utilizes FBG sensor. She can be contacted at email: marmoh\_1968@uomustansiriyah.edu.iq.